J|A|C|S ARTICLES

Published on Web 08/10/2009

A Mechanistic Investigation on Copolymerization of Ethylene with Polar Monomers Using a Cyclophane-Based Pd(II) α-Diimine Catalyst[1]

Chris S. Popeney and Zhibin Guan*

Department of Chemistry, University of California, 1102 Natural Sciences 2, Irvine, California 92697

Received June 2, 2009; E-mail: zguan@uci.edu

Abstract: A detailed mechanistic investigation of the copolymerization of ethylene and methyl acrylate (MA) by a Pd(II) cyclophane-based α-diimine catalyst is reported. Our previous observations of unusually high incorporations of acrylates in copolymerization using this catalyst (*J. Am. Chem. Soc.* **2007**, *129*, 10062) prompted us to conduct a full mechanistic study on ethylene/MA copolymerization, which indicates a dramatic departure from normal Curtin−Hammett kinetic behavior as observed in copolymerization using the normal Brookhart type of Pd(II) α-diimine catalysts. Further investigation reveals that this contrasting behavior originates from the axial blocking effect of the cyclophane ligand hindering olefin substitution and equilibration. In equilibrium studies of ethylene with nitriles, the cyclophane catalyst was found to more strongly favor the linearly binding nitrile ligands as compared to the standard acyclic Pd(II) α-diimine catalysts. Ethylene exchange rates in the complexes $[(N\hat{}N)PdMe(C_2H_4)]^+$ (N^N = diimine) were measured by 2D EXSY NMR spectroscopy and found to be over 100 times slower in the cyclophane case. Measurement of the slow equilibration of ethylene, methyl acrylate, and 4-methoxystyrene in cyclophane-based Pd(II) olefin complexes by ^{1}H NMR and fitting of the obtained kinetic plots allowed for the estimation of exchange rates and equilibrium constants of the olefins. After extrapolation to typical polymerization temperature, $\Delta G^{\ddagger} =$ 20.6 and 16.4 kcal/mol for ethylene-methyl acrylate exchange in the forward (ethylene displacement by methyl acrylate) and reverse directions, respectively. These values are of similar magnitude to the previously determined migratory insertion barriers of ethylene ($\Delta G^{\ddagger} = 18.9$ kcal/mol) and methyl acrylate ($\Delta G^{\ddagger} = 16.3$ kcal/mol) under equivalent conditions, but contrast strongly to the rapid olefin exchange seen in the Brookhart acyclic catalyst. The large barrier to olefin exchange hinders olefin pre-equilibrium, decreasing the cyclophane catalyst's ability to preferentially incorporate one monomer (in this case ethylene) over the other, thus giving rise to high comonomer incorporations.

Introduction

Transition metal catalyzed copolymerization of ethylene with polar-functionalized olefins is a highly attractive but challenging endeavor. In the past decade or so, interest has intensified dramatically as a large body of new work involving olefin polymerization catalyst systems utilizing late transition metals has been published.[2−6] A series of cationic Pd(II) α-diimine-based catalysts, reported by Brookhart and co-workers, were the first successful systems able to copolymerize important polar feedstock monomers, like acrylates, with ethylene.[7,8] Since then, neutral Ni(II) and Pd(II) catalyst systems have shown particular promise because of their superior functional group tolerance,[3,9−11] permitting copolymerizations in water,[12] the incorporation of notoriously difficult comonomers like acrylonitrile,[13] and incorporations of acrylates in excess of 50%.[14] Copolymerizations with the cationic Pd(II) α-diimine catalysts like **1** (Chart 1), however, have been more thoroughly investigated by mechanistic[15] and computational[16,17] studies. Brookhart and co-workers discovered that the incorporation ratio of methyl

(1) This paper has been adapted in part from the following thesis: Ph.D. Dissertation. University of California at Irvine, CA. Popeney, C. S. 2008.
(2) Ittel, S. D.; Johnson, L. K.; Brookhart, M. *Chem. Rev.* **2000**, *100*, 1169–1203.
(3) Younkin, T. R.; Connor, E. F.; Henderson, J. I.; Friedrich, S. K.; Grubbs, R. H.; Bansleben, D. A. *Science* **2000**, *287*, 460–462.
(4) Boffa, L. S.; Novak, B. M. *Chem. Rev.* **2000**, *100*, 1479–1493.
(5) Gibson, V. C.; Spitzmesser, S. K. *Chem. Rev.* **2003**, *103*, 283–315.
(6) Small, B. L.; Brookhart, M. *J. Am. Chem. Soc.* **1998**, *120*, 7143–7144.
(7) Johnson, L. K.; Killian, C. M.; Brookhart, M. *J. Am. Chem. Soc.* **1995**, *117*, 6414–6415.
(8) Johnson, L. K.; Mecking, S.; Brookhart, M. *J. Am. Chem. Soc.* **1996**, *118*, 267–268.
(9) Hicks, F. A.; Brookhart, M. *Organometallics* **2001**, *20*, 3217–3219.
(10) Drent, E.; van Dijk, R.; van Ginkel, R.; van Oort, B.; Pugh, R. I. *Chem. Commun.* **2002**, 744–745.
(11) Luo, S.; Vela, J.; Lief, G. R.; Jordan, R. F. *J. Am. Chem. Soc.* **2007**, *129*, 8946–8947.
(12) Gottker-Schnetmann, I.; Korthals, B.; Mecking, S. *J. Am. Chem. Soc.* **2006**, *128*, 7708–7709.
(13) Kochi, T.; Noda, S.; Yoshimura, K.; Nozaki, K. *J. Am. Chem. Soc.* **2007**, *129*, 8948–8949.
(14) Guironnet, D.; Roesle, P.; Ruenzi, T.; Goettker-Schnettmann, I.; Mecking, S. *J. Am. Chem. Soc.* **2009**, *131*, 422–423.
(15) Mecking, S.; Johnson, L. K.; Wang, L.; Brookhart, M. *J. Am. Chem. Soc.* **1998**, *120*, 888–899.
(16) Michalak, A.; Ziegler, T. *J. Am. Chem. Soc.* **2001**, *123*, 12266–12278.
(17) Szabo, M. J.; Jordan, R. F.; Michalak, A.; Piers, W. E.; Weiss, T.; Yang, S.-Y.; Ziegler, T. *Organometallics* **2004**, *23*, 5565–5572.

10.1021/ja904471v CCC: $40.75

Chart 1. Acyclic (**1**) and Cyclophane-Based (**2**) α-Diimine Pd(II) Olefin Polymerization Catalysts

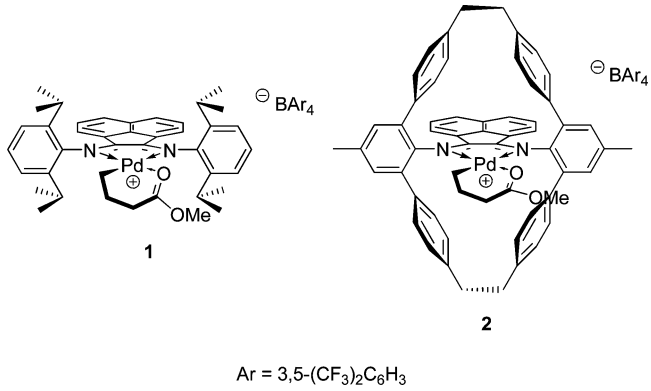

Ar = 3,5-$(CF_3)_2C_6H_3$

Scheme 1. Curtin−Hammett-Based Model of Ethylene−Acrylate Copolymerization with Catalyst **1** (ref 15)

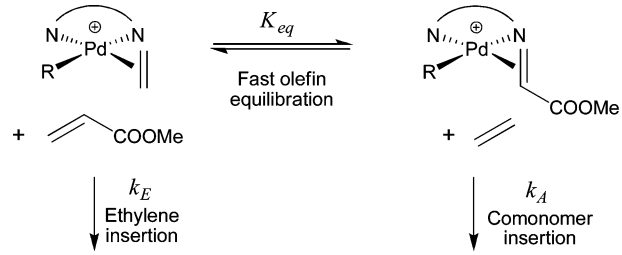

acrylate follows the standard Curtin−Hammett relationship, given in eq 1.[15] By this mechanism, both metal−ethylene and metal−acrylate complexes are in rapid equilibrium while the migratory insertion of monomer into the growing polymer chain takes place comparatively slowly (Scheme 1). The ratio of monomer incorporation is dependent upon the relative rates of ethylene and acrylate insertion, given by rate constants k_E and k_A, and the equilibrium constant K_{eq} of complexation of the two olefins. The incorporation of acrylates by these catalysts was low, a result of the far higher coordination strength of ethylene compared to MA.

$$\left(\frac{[\text{Acrylate}]}{[\text{Ethylene}]}\right)_{\text{Polymer}} = K_{eq}\frac{k_A[\text{A}]}{k_E[\text{E}]} \qquad (1)$$

In order to address general shortcomings of the cationic α-diimine-based catalysts, namely their sensitivity at high temperature,[18,19] our laboratory prepared a new class of Ni(II) and Pd(II) catalysts bearing an α-diimine ligand with a cyclic cyclophane-type structure.[20] Presumably due to the conformational inflexibility of the closed rigid cyclophane ligand presenting groups that severely hinder access to the axial metal coordination sites, these catalysts have exhibited thermal stabilities significantly higher than the original acyclic α-diimine catalysts. Polymerizations at elevated temperature with the cyclophane catalysts afforded polyolefins of higher molecular weight, believed to result from a reduction in the rate of associative chain transfer processes.[21]

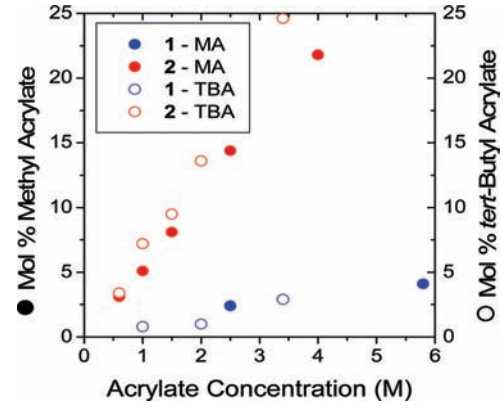

Figure 1. Incorporation ratio of MA and TBA into copolymer from catalysts **1** and **2** (ref 22).

Table 1. Ethylene Homopolymerizations and Copolymerizations with Methyl Acrylate Using Catalysts **1** and **2** (ref 22)[a]

				TON					
entry	cat.	[MA] (mol/L)	yield (mg)	C_2H_4	MA	mol % MA[b]	M_n (kg/mol)[b]	M_w/M_n[c]	B[d]
1	**1**	0[e]	6600	23500	−	−	33.7	1.54	101
2	**1**	1.0	340	1200	10	**0.8**	26.8	1.48	104(105)
3	**1**	2.5	120	400	10	**2.4**	19.3	1.51	100(108)
4	**1**	5.8	80	270	11	**4.1**	7.3	1.61	97(112)
5	**2**	0[e]	2280	8100	−	−	12.9	1.68	106
6	**2**	1.0	100	310	16	**5.1**	10.1	1.35	96(114)
7	**2**	2.5	30	70	12	**14.4**	8.03	1.35	72(130)
8	**2**	4.0	30	60	16	**21.8**	6.67	1.18	71(153)

[a] Polymerization conditions: 10.0 μmol of catalyst, 88 psi ethylene pressure, 35 °C, 18 h. [b] Determined by ^{1}H NMR. [c] Determined by SEC-MALS. [d] Branching density per 1000 carbons determined by ^{1}H NMR. Values in parentheses include ester groups as chain ends. [e] Ethylene homopolymerizations shown for comparison.

Quite unexpectedly, we discovered that the cyclophane-based Pd(II) α-diimine catalyst **2** could incorporate both methyl acrylate (MA) and *tert*-butyl acrylate (TBA) monomers in copolymerizations with ethylene far more effectively than the corresponding acyclic catalyst **1** (Figure 1).[22] Copolymers with molar ratios of acrylate above 20%, nearly 5 times the maximum incorporation level observed in polymerizations with acyclic Pd(II) α-diimine catalyst **1**,[15] were produced (Table 1). The rate constant ratios of ethylene and MA insertion (k_E/k_A) were measured for each catalyst, but the values were similar within experimental error. This implies that the enhanced efficiency for acrylate incorporation for the cyclophane catalyst is not due to the change of relative insertion barrier caused by the new ligand framework. From eq 1, perturbation of the monomer binding equilibrium could also have explained the excess of MA incorporation. The direct measurement of ethylene−MA exchange equilibrium constants was not possible with catalyst **2**, however, because of the apparently low reactivity of the cyclophane Pd(II) complex to ligand substitution.

In accordance with reduced rates of associative chain transfer, suppression by the cyclophane ligand of associative substitution was hypothesized to account for the unexpectedly high acrylate incorporation ability. Retardation of fast olefin equilibrium, we reasoned, would reduce the selectivity of the metal to the monomers based on their binding strengths, rendering the Curtin−Hammett assumption invalid and permitting an over-

(18) Gates, D. P.; Svejda, S. K.; Onate, E.; Killian, C. M.; Johnson, L. K.; White, P. S.; Brookhart, M. *Macromolecules* **2000**, *33*, 2320–2334.
(19) Tempel, D. J.; Johnson, L. K.; Huff, R. L.; White, P. S.; Brookhart, M. *J. Am. Chem. Soc.* **2000**, *122*, 6686–6700.
(20) Camacho, D. H.; Salo, E. V.; Ziller, J. W.; Guan, Z. *Angew. Chem., Int. Ed.* **2004**, *43*, 1821–1825.
(21) Camacho, D. H.; Guan, Z. *Macromolecules* **2005**, *38*, 2544–2546.
(22) Popeney, C. S.; Camacho, D. H.; Guan, Z. *J. Am. Chem. Soc.* **2007**, *129*, 10062–10063.

Chart 2. Pd(II) α-Diimine Methyl Complexes Used in Mechanistic Studies

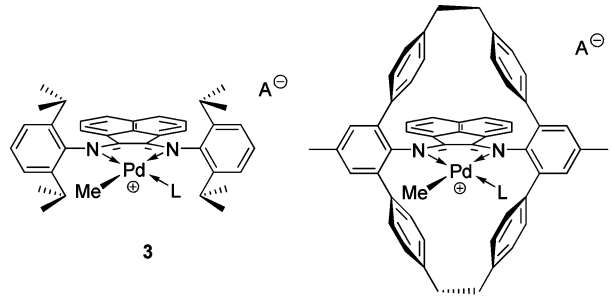

a: L = Et_2O or H_2O, A^- = SbF_6^-
b: L = C_2H_4, A^- = SbF_6^-
c: L = $C_2H_3(CO_2Me)$, A^- = SbF_6^-
d: L = $C_2H_3(4\text{-}OMeC_6H_4)$, A^- = SbF_6^-
e: L = MeCN, A^- = BAr_4^-
f: L = CH_2ClCN, A^- = BAr_4^-

Scheme 2. Ligand Exchange in Pd(II) Complexes

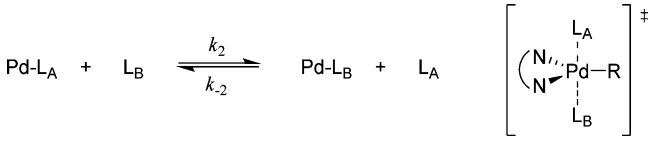

incorporation of acrylate. Since our initial communication,[22] we have carried out a detailed mechanistic and kinetic investigation using one-dimensional and two-dimensional NMR methods on a series of cyclophane-based Pd(II) olefin complexes (Chart 2). The exchange rates of olefins were measured and the energetic barriers to exchange processes were compared to the barriers of migratory insertion. The results reveal that olefin exchange by associative substitution is dramatically suppressed by the presence of the cyclic cyclophane ligand of **2**, resulting in a decrease of the cyclophane catalyst's ability to preferentially incorporate one monomer (in this case ethylene) over the other, thus giving rise to high comonomer incorporations.

Experimental Section

General Considerations. NMR spectra were recorded on Bruker DRX400 and DRX500 FT-NMR instruments. Proton and carbon NMR spectra were recorded in ppm and were referenced to indicated solvents. Data was reported as follows: chemical shift, multiplicity (s = singlet, d = doublet, t = triplet, q = quartet), integration, and coupling constant(s) in Hertz (Hz). Multiplets (m) were reported over the range (ppm) at which they appear at the indicated field strength. All synthetic procedures, including the preparation and characterization of new complexes **4e** and **4f** and additional details regarding substance preparation and handling, is described in the Supporting Information.

Kinetic Treatment. Ligand substitution (Scheme 2) at square planar d^8 complexes, such as Pd(II), is widely held to proceed by an associative mechanism.[23,24] Associative chain transfer has been proposed by Brookhart, for example, to proceed through a 5-coordinate transition state,[19] as should the exchange of olefins prior to monomer insertion (Scheme 2). The rate of such a process is dependent on the concentrations of the free olefins as well as the Pd(II) complexes. The second-order rate law is shown in eq 2, where k_2 and k_{-2} are the forward and reverse rate constants, respectively.

$$-\frac{\mathrm{d}[\mathrm{PdL_A}]}{\mathrm{d}t} = k_2[\mathrm{PdL_A}][\mathrm{L_B}] - k_{-2}[\mathrm{PdL_B}][\mathrm{L_A}] \qquad (2)$$

Addition of a second olefin L_B to a solution of a Pd(II) complex of olefin L_A (or PdL_A) results in the equilibration of the system following the general second-order rate law given in eq 2. If the concentrations of each free ligand is in a large enough excess compared to the Pd complex with which it is paired in the terms of eq 2, the pseudo-first-order approximation may be applied to allow simplification to eq 3, where k_1 and k_{-1} are the pseudo-first-order rate constants.[25] Integration then affords eqs 4 and 5, where x_{eq} is the change in concentration of all species during equilibration, or the departure from equilibrium (eq 6). Equations 4 and 5, respectively, describe the time-dependent concentration of the complexes PdL_A and PdL_B as functions of the equilibrium concentrations, x_{eq}, and the sum of the rate constants k_1 and k_{-1}. The pseuso-first-order approximation is valid in the regime where x_{eq} is small, meaning at small departures from equilibrium, compared to the actual concentrations of the complexes and free ligands.[25]

$$-\frac{d[\mathrm{PdL_A}]}{dt} = k_1[\mathrm{PdL_A}] - k_{-1}[\mathrm{PdL_B}] \qquad (3)$$

$$[\mathrm{PdL_A}](t) = [PdL_A]_{\mathrm{eq}} + x_{eq}\, e^{-(k_1+k_{-1})t} \qquad (4)$$

$$[PdL_B](t) = [PdL_B]_{eq} - x_{eq}\mathrm{e}^{-(k_1+k_{-1})t} \qquad (5)$$

$$\begin{aligned} x_{eq} &= [PdL_A]_0 - [PdL_A]_{\mathrm{eq}} \\ &= [PdL_B]_{\mathrm{eq}} - [PdL_B]_0 \end{aligned} \qquad (6)$$

Following the introduction of the second olefin, the concentrations of all species were monitored over a period of up to eight hours at low temperature by ^{1}H NMR. The concentrations of the complexes were plotted as functions of time and the curves fitted to a first-order exponential function[26,27] in the form of eqs 4 or 5 by the Origin software program. In this manner, the exchange rate constants and the equilibrium concentrations could be calculated. In order to ensure the validity of the pseudo-first-order approximation, only measurements made at later time, in which the concentration of free ligand was at least 5 times higher than the concentration of the complex existing in the same term as eq 2, were included in the fit. In practice, these conditions were realized by using a large excess (at least 10-fold) of the weakly binding ligand L_A and then adding approximately a 3-fold excess of the strongly binding ligand L_B. Only data points following ~70% equilibration were used in calculations. The concentrations of species in these experiments are tabulated in the Supporting Information, Tables S2, S3, and S4. It can be seen that the concentrations of the free ligands are at least 5 times the concentration of the Pd complex and reach far higher ratios at later equilibration times, indicating that the pseudo-first-order approximation is valid.

(23) Crabtree, R. H. *The Organometallic Chemistry of the Transition Metals*, 3rd ed.; John Wiley and Sons, Inc: New York, 2001.
(24) Shriver, D. F.; Atkins, P. W. *Inorganic Chemistry*, 3rd ed.; W. H. Freeman and Company: New York, 1999.
(25) Houston, P. L. *Chemical Kinetics and Reaction Dynamics*; McGraw-Hill: New York, 2001.
(26) Eigen, M. *Discuss. Faraday Soc.* **1954**, *17*, 194–205.
(27) Bracken, D. E.; Baldwin, H. W. *Inorg. Chem.* **1974**, *13*, 1325–1329.

In the simple case of the exchange of bound ethylene with free ethylene, eq 2 can be rewritten as eq 7, where k_2 is the second-order rate constant. Equation 7 describes the total amount of exchange "events", which can be detected in dynamic NMR methods such as EXSY by the transfer of magnetization that occurs. Since this system is in dynamic equilibrium and the concentrations of all species remain constant, the pseudo-first-order approximation may be applied, affording eqs 8 and 9. The pseudo-first-order rate constants k_1 and k_{-1} could then be related to k_2 by eqs 10 and 11, respectively.

$$\text{rate} = k_2[\text{Pd}(\text{C}_2\text{H}_4)][\text{C}_2\text{H}_4] \tag{7}$$

$$= k_1[\text{Pd}(\text{C}_2\text{H}_4)] \tag{8}$$

$$= k_{-1}[\text{C}_2\text{H}_4] \tag{9}$$

$$k_1 = k_2[\text{C}_2\text{H}_4] \tag{10}$$

$$k_{-1} = k_2[\text{Pd}(\text{C}_2\text{H}_4)] \tag{11}$$

Low-Temperature One-Dimensional ^{1}H NMR Experiments. A 10 ppm spectral window was used, and irradiation was centered at 4.5 ppm. A single 90° pulse was performed, preceded by at least a 60 s delay, with an 8.0 s acquisition time. If possible, the probe was tuned to optimize sensitivity at the measurement temperature. The duration between acquisitions in kinetic studies was adjusted by changing the delay.

Measurement of Ethylene Exchange Rates by EXSY NMR. (1) Acquisition Parameters. A standard gradient NOESY pulse sequence was employed in the EXSY experiments, with a spectral width of 2.0 ppm, an offset of 4.8 ppm, 128 experiments in the F1 domain with two scans each, and delays of 2 s between each scan (approximate experiment time was 15 min). Since the two exchanging sites in this studied system lie on different molecular species (and are therefore far apart), it can be assumed only exchange processes contributed to the transfer of magnetization.

(2) Experimental Setup. Sets of experiments, conducted at specific temperature and concentration conditions, consisted of a reference EXSY experiment with mixing time set to zero and two or three experiments of varying mixing times t_m, all under specific temperature and concentration conditions. To account for sample or spectrometer drift during the sets, one-dimensional spectra (using standard low temperature parameters) were acquired before all EXSY runs to permit the measurement of the exact concentration of species by comparison to a known amount of added diphenylmethane standard. These experiment sets were acquired at four different concentrations of free ethylene at constant temperature to measure the concentration dependence of k_1. Additionally, sets were acquired at two other temperatures, at highest or lowest ethylene concentrations in the case of the cyclophane or acyclic system, respectively, to measure the temperature dependence of k_1. The intensity of diagonal and cross-peaks in the EXSY spectra were obtained by volume integration following appropriate phase and baseline correction. Regions of both positive and negative intensity were included in the integration to minimize the effect of baseline noise.

(3) Determination of Rate Constants. The EXSYCalc software package, available online at www.mestrec.com, was used to determine the pseudo-first-order rate constants k_1 and k_{-1}. The intensities of the diagonal peaks and cross-peaks are divided by the peak intensities of the reference spectrum. The program then evaluates the rate matrix **R**,[28] the diagonal terms of which are related to the T_1 relaxation of each site and the exchange rates while the off-diagonal elements are the rate constants k_1 and k_{-1}. The second-order rate constant k_2 was determined from the plot of ethylene concentration dependence on k_1, where the slope of the linear fit is equal to k_2. Under the assumption the temperature dependence of k_2 was equal to the temperature dependence of k_1, the activation parameters of exchange $\Delta H^{\ddagger}$ and $\Delta S^{\ddagger}$ were then calculated from the Eyring plot of k_2, allowing for extrapolation of exchange rates to polymerization temperature.

(4) Mixing Time Consideration. As t_m increases, the cross-peak intensity increases in a linear manner. At some point, however, T_2 relaxation mechanisms begin to affect magnetization transfer and the linear correlation is affected.[28] Thus t_m should be chosen to be small enough so that the cross-peak intensities are still increasing linearly but large enough that cross-peaks are large enough to be accurately measured.[29] In the case of the acyclic catalyst, exchange was fast enough that short values of t_m of 10 to 20 ms, well within the linear growth region, could suffice to give intense cross-peaks. With the cyclophane catalyst, longer mixing times, from 100 to 800 ms, were necessary because of the slower exchange of the system. This corresponds well to the optimal mixing time of about 420 ms according to the formula below,[28] calculated using T_1 of the Pd

$$t_{m,opt} \approx \frac{1}{T^{-1} + k_1 + k_{-1}}$$

complex (0.45 s). Values of k_1, calculated from different mixing times, were plotted versus ethylene concentration (as in the determination of k_2), and the mixing times corresponding to the best linear fits were selected (see the Supporting Information, Table S1). Longer mixing times were found to give best results.

(5) Error Analysis. Errors in k_2, δk_2, were calculated from the linear fit of the k_1 versus $[\text{C}_2\text{H}_4]$ plot by the least squares method. To propagate this error to the temperature dependence measurements, two new values of k_2 equal to $k_2 \pm \delta k_2$ were determined. In addition to k_2, values of $k_2 \pm \delta k_2$ proportional to the temperature dependence of k_1 were calculated at the other two temperatures. An Eyring plot consisting of $k_2 + \delta k_2$, k_2, and $k_2 - \delta k_2$ for the three temperatures was constructed, and errors in $\Delta H^{\ddagger}$ and $\Delta S^{\ddagger}$ were calculated from the linear fit by the least squares method.

Ligand Equilibration Studies. An NMR tube was charged with 10 μmol of complex **3a** or **4a** under nitrogen atmosphere and closed with a septum cap. The tube was precooled in the instrument to −100 °C, and 0.6 mL of CD_2Cl_2 was added along with a known amount of an internal standard: diphenylmethane (s, δ 3.95 ppm) in studies with ethylene or 1,2,2,3-tetrachloropropane (s, δ 4.15 ppm) for experiments with MA. The more weakly binding ligand was added in large excess followed by a 30 min period of equilibration during which its complexation took place. A spectrum was acquired by the standard low temperature acquisition parameters. The stronger binding ligand was added later, the temperature was adjusted as desired, and a loop routine was used to carry out the time-lapsed kinetic study, with delay increased to the desired time interval between experiments and the standard acquisition parameters used. The more weakly binding olefin was usually added in far larger amounts to allow for a measurable equilibration. Displacement of the first olefin by the second was rapid for the acyclic catalyst system but required many hours for the cyclophane system for all cases except experiments involving nitriles, which equilibrated completely within one hour. Following the experiment, an external anhydrous methanol standard was used to accurately determine the experiment temperature. Concentrations of the Pd-bound species were determined by peak height measurements of the corresponding Pd−Me resonances normalized to the intensity of the internal standard. Equilibrium constants were measured from the concentration of Pd adducts and free olefins at equilibration. A five percent error was assumed in all peak height measurements.

(28) Perrin, C. L.; Dwyer, T. J. *Chem. Rev.* **1990**, *90*, 935–967.

(29) Dimitrov, V. S.; Vassilev, N. G. *Magn. Reson. Chem.* **1995**, *33*, 739–744.

Table 2. Equilibrium Constants and Energetic Parameters of Ethylene−Nitrile Exchange for Acyclic (**3**) and Cyclophane-Based (**4**) Pd(II) Complexes Based on the Mechanism in Scheme 2

entry	diimine series	L_A-L_B	T (K)	K_{eq}	ΔG (kcal/mol)	ΔH (kcal/mol)[b]	ΔS (kcal/mol)[b]
1	**3**	MeCN−C_2H_4	190	0.27 ± 0.02	0.49 ± 0.02		
2	**3**	MeCN−C_2H_4	208	0.24 ± 0.02	0.58 ± 0.03	0.38 ± 0.12	−4.7 ± 0.6
3	**3**	MeCN−C_2H_4	224	0.23 ± 0.02	0.66 ± 0.03		
4	**4**	$CH_2ClCN-C_2H_4$	190	$(3.9 \pm 0.3) \times 10^{-3}$	2.1 ± 0.1		
5	**4**	$CH_2ClCN-C_2H_4$	208	$(4.1 \pm 0.3) \times 10^{-3}$	2.2 ± 0.1	0.40 ± 0.08	−8.9 ± 0.4
6	**4**	$CH_2ClCN-C_2H_4$	224	$(4.6 \pm 0.4) \times 10^{-3}$	2.4 ± 0.1		
7	**4**	MeCN−CH_2ClCN	190	0.040 ± 0.003	1.2 ± 0.1		
8	**4**	MeCN−CH_2ClCN	224	0.048 ± 0.004	1.4 ± 0.1	0.32 ± 0.06	−4.7 ± 0.2
9	**4**	MeCN−CH_2ClCN	298	0.055 ± 0.004	1.7 ± 0.1		
10	**4**	MeCN−C_2H_4	190	$(1.5 \pm 0.3) \times 10^{-4}$[c]	3.3 ± 0.2[c]	0.72 ± 0.14[d]	−13.6 ± 0.6[d]
11	**4**	MeCN−C_2H_4	224	$(2.2 \pm 0.4) \times 10^{-4}$[c]	3.8 ± 0.2[c]		

[a] Determined by ^{1}H NMR. Solvent = CD_2Cl_2. [b] Calculated from plots of ln K_{eq} versus $1/T$. [c] Calculated from the products of K_{eq} from CH_2ClCN/C_2H_4 and $MeCN/CH_2ClCN$ experiments at given temperature. [d] Caluclated from ΔH and ΔS values for entries 4−6 and 7−9.

For slowly equilibrating systems, the equilibrium constant and the pseudo-first-order exchange rate constants were derived by fitting eqs 4 or 5 to plots of the concentrations of the Pd-bound species with time. Errors in exchange rates were calculated from the exponential fits by the least-squares method.

Results

The preparation of cyclophane-based Pd(II) methyl cationic complexes with a labile ligand for use in NMR investigations has been previously described. The complexes involved in mechanistic studies are shown in Chart 2, which include the acyclic ether complex **3a**[8] and cyclophane-based water complex **4a**.[22] The complexation of olefins was then performed *in situ* as necessary for NMR experiments by addition of the gaseous or liquid olefin into a cooled solution of **3a** or **4a** in CD_2Cl_2 affording the ethylene, MA, and 4-methoxystyrene (MS) adducts **3b/4b**, **3c/4c**, and **3d/4d**, respectively.

Equilibration of Nitriles and Olefins. Late transition metal complexes containing a nitrile ligand can be conveniently prepared and are relatively stable; therefore, we began our investigation with nitrile complexes. Acetonitrile complexes of Pd(II) bearing the acyclic or cyclophane-based α-diimine ligands, **3e** and **4e**, respectively, were studied in pairwise NMR experiments with ethylene. The calculated equilibrium constants from various ligand pairs are shown in Table 2 for the acyclic (**3**) and cyclophane-based (**4**) catalysts. The results of nitrile−ethylene equilibration show that the cyclophane catalyst exhibited a 3 orders of magnitude greater preference toward the binding of nitrile instead of ethylene as compared to the acyclic catalyst (Table 2, entries 3 and 10). Because ethylene displacement of acetonitrile was too weak to measure directly by ^{1}H NMR in the cyclophane system, the displacement of more weakly binding chloroacetonitrile from the adduct **4f** (entries 4−6 and 7−9, respectively), was used to compute the C_2H_4−MeCN equilibrium constant for comparison to that of the acyclic catalyst.

The temperature dependence on K_{eq} was then used to determine ΔH and ΔS of the equilibrium process. Concerning ΔH, displacement of acetonitrile by ethylene is almost thermoneutral for both the acyclic and cyclophane catalysts. However, the entropic change is much more pronounced for the cyclophane catalyst as compared to the acyclic one. The strongly negative ΔS value of −13.6 cal/mol*K for the cyclophane catalyst suggests that the ethylene complex **4b** is highly ordered compared to acetonitrile adduct **4e**. This can be attributed to steric interactions that exist between the preferred conformation of the bound olefin and the bulky cyclophane ligand. Olefins are well-known to bind to metals through an $\eta^2-\pi$-type interaction, in which the olefin C−C bond is oriented perpendicular to the metal coordination plane. Compared to a linear, η^1 σ-donating ligand like acetonitrile, the accommodation of ethylene in the sterically encumbered cyclophane complex should be significantly more demanding. To illustrate this point, a simple model of ethylene complex **4b** derived from semiempirical calculations was constructed (Figure 2).[30] The olefin can be seen coordinating to the metal from within a binding pocket formed by the specific orientation of the cyclophane phenyl rings.

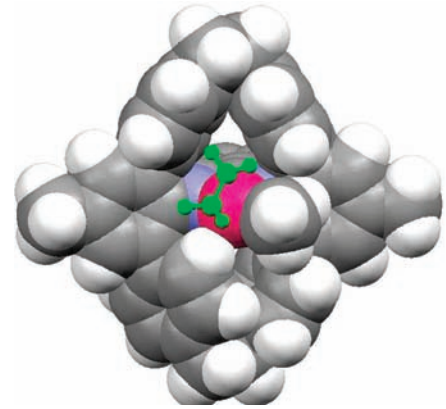

Figure 2. PM3 model of cation **4b** showing the ethylene ligand in green. Palladium is magenta, carbon is black, nitrogen is blue, and hydrogen is white.

Rates of Ethylene Exchange. The simplest olefin exchange scenario, the exchange of free and bound ethylene, was first examined for both the acyclic and cyclophane Pd(II) catalysts. In our previous study, attempts to measure the rate of ethylene exchange for the cyclophane system, important in testing the applicability of the Curtin−Hammett principle, were not successful.[22] In the current investigation, exchange was observed between free ethylene and cyclophane-based ethylene complex **4b** by two-dimensional exchange spectroscopy, or EXSY NMR.[28]

The EXSY technique provided the pseudo-first-order rate constants k_1 and k_{-1} from experiments with the acyclic complex **3b** as well as cyclophane complex **4b**. Details of data acquisition

(30) The equilibrium geometry of cyclophane ethylene adduct **4b** was generated by the Spartan software package (Wavefunction, Inc., of Irvine, CA). The structure of the methyl chloride complex obtained from X-ray crystallography (ref 20) was imported, the chloride ligand removed, and an ethylene molecule substituted. Semi-empirical calculations (PM3) were performed, which converged to the shown structure regardless of the starting configuration of the olefin (whether in or perpendicular to the metal coordination plane).

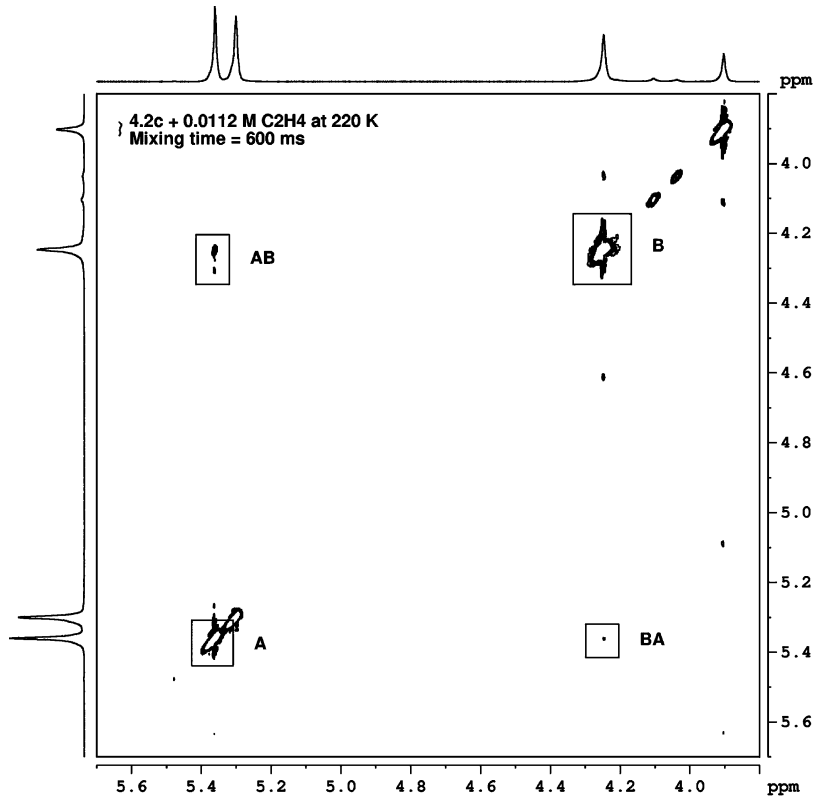

Figure 3. EXSY with 600 ms mixing time for the cyclophane adduct of ethylene **4b** at 220 K. The signals at 5.30 and 3.95 ppm are dichloromethane and diphenylmethane, respectively.

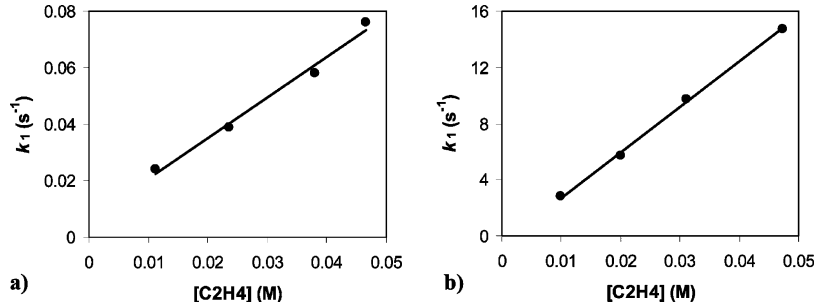

Figure 4. Plot of ethylene exchange rate constant k_1 versus free ethylene concentration for (a) the acyclic complex **3b** at 190 K and (b) the cyclophane-based complex **4b** at 220 K. The slope of the linear fit is the second-order rate constant k_2.

and data analysis can be found above in the experimental section. The results of the EXSY experiments for cyclophane ethylene complex **4b** under various reaction conditions and mixing times, t_m, are tabulated in the Supporting Information, Table S1. Rate constants were calculated by the program EXSYCalc from comparison of diagonal and cross-peak volumes for a spectrum at selected t_m to those from a reference spectrum with t_m set to zero under the same conditions. The rate constant k_1 was directly related to the concentration of free ethylene, as expected for a second-order process and eq 10. Constant k_{-1}, however, remained nearly unchanged (aside from its temperature dependence) owing to its dependence from eq 11 on the concentration of Pd(II) complex, which was not varied in these experiments.

A representative EXSY spectrum obtained for the cyclophane complex **4b**, along with the regions of integration, is shown in Figure 3. As can be seen, the crosspeaks were weak as a result of the slow exchange kinetics but, nevertheless, still visible. An accurate value of the second-order rate constant k_2 was calculated from the slope of a plot of measured k_1 at different concentrations of free ethylene. The calculated values of k_2 were 1.4 ± 0.1 $s^{-1}M^{-1}$ and 320 ± 10 $s^{-1}M^{-1}$ for the cyclophane system **4b** at 220 K and the acyclic system **3b** at 190 K, respectively. Plots of k_1 versus ethylene concentration and the linear fits are shown in Figure 4. The strong dependence of k_1 on ethylene concentration illustrates the associative nature of the exchange.

By measurement of k_1 at different temperatures, its temperature dependence was determined. Because k_1 and k_2 have the same temperature dependence, the respective values of k_2 at each temperature could be determined from k_1 at those temperatures. The Eyring plots of ethylene exchange for both the cyclophane and acyclic catalyst are shown in Figure 5. The following activation parameters for ethylene exchange were calculated from the Eyring plot of the acyclic system: $\Delta H^{\ddagger} = 2.5 \pm 0.1$ kcal/mol, $\Delta S^{\ddagger} = -33 \pm 1$ cal/mol*K. Extrapolation

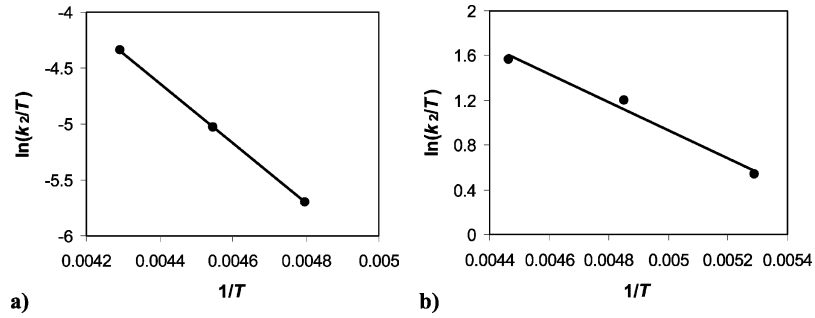

Figure 5. Eyring plot of ethylene exchange for (a) the acyclic complex **3b** and (b) the cyclophane-based complex **4b**.

to the polymerization temperature (35 °C) gives $\Delta G^{\ddagger} = 12.6 \pm 0.3$ kcal/mol. For the cyclophane system, the same treatment led to the following activation parameters: $\Delta H^{\ddagger} = 5.3 \pm 0.2$ kcal/mol, $\Delta S^{\ddagger} = -33 \pm 1$ cal/mol*K, and $\Delta G^{\ddagger} = 15.5 \pm 0.4$ kcal/mol at 35 °C. The enthalpies of activation are markedly different in both catalyst systems. The significantly higher $\Delta H^{\ddagger}$ for ethylene exchange with the cyclophane system leads to the far slower exchange rates of ethylene, over 2 orders of magnitude slower than the acyclic catalyst. This phenomenon is most likely due to the increased steric blocking effect of the cyclophane ligand. The large negative and nearly identical values of $\Delta S^{\ddagger}$ for both systems confirm that the exchange of ethylene, and most likely the other olefins as well, proceeds by the associative ligand substitution mechanism. Consequentially, the cyclophane ligand, with its axial steric bulk, greatly decreases the rate of substitution processes.

Exchange Rates of Ethylene with Other Olefins. Olefin equilibration was monitored by ^{1}H NMR analysis in CD_2Cl_2 at temperatures below olefin insertion rates. Ethylene binds to Pd(II) so much more strongly than does MA that the ethylene−MA equilibrium constant was unable to be determined from a simple ethylene−MA pairwise experiment. As in Brookhart's study,[15] 4-methoxystyrene (MS) was employed as an olefin of complexation strength between that of ethylene and MA to aid in the measurement of the ethylene−MA equilibrium constant. Attempted measurements of the equilibrium constants for olefins at low temperature with the cyclophane catalyst, however, were complicated by the extremely slow exchange rates that were apparent. Several hours were often not sufficient to reach full equilibrium, placing unreasonable demands on instrument time. As an alternative strategy using the pseudo-first-order approximation, the time-dependent plots of the concentration of Pd−olefin species were fitted to first-order exponential functions and the equilibrium concentrations and exchange rate constants thereby derived.[26,27] Details of the data analysis are provided above in the Experimental Section, along with our rationale in applying the pseudo-first-order approximation. The concentrations of species present in the NMR experiments are also tabulated in the Supporting Information.

The equilibrium constants for the olefin pairs ethylene−MS and MS−MA with the cyclophane system were calculated by fitting the plots of Pd(II) complex concentration to eqs 4 or 5 (Figure 6), allowing for the determination of the concentrations of the species at equilibrium. Fit correlations were of high quality, with values of R^2 at least 0.996 for all equilibrating complexes. Evaluation of the exchange rate constants, in the form of the sum $k_1 + k_{-1}$, was also performed by the fit. All olefin equilibration data is compiled in Table 3. In contrast to the cyclophane system, the acyclic system equilibrated too rapidly for its progress to be effectively monitored and exchange rate constants to be determined. Although an equilibrium constant was obtained for the ethylene−MS pair, the Pd−Me signals were obscured by ligand resonances in the MS−MA experiment. Instead, the previously reported values using a similar acyclic ligand are given for the MS−MA and the overall ethylene−MA equilibria (see Table 3, footnote d).

While the calculated ethylene−MS equilibrium constant for the cyclophane system was similar to that of the acyclic catalyst, the MS−MA equilibrium constant was significantly higher. From the product of K_{eq} from both pairs (Table 3, entries 4 and 5), the ethylene−MA equilibrium constant was determined to be 2.7×10^{-5} at 202 K. If ΔS of equilibrium is assumed to be negligible, the equilibrium constant is then estimated to be 1.0×10^{-3} when extrapolated to 35 °C, or about 3−4 times higher (favoring MA complexation) in the cyclophane catalyst than in the acyclic catalyst. Although this favorable complexation of MA could partially contribute to the larger incorporation of MA by the cyclophane catalyst, the slow ligand exchange rates deserve further consideration. The exchange rates for both olefin pairs calculated from the fits were found to be extremely slow for the cyclophane complex. Lastly, the rate of ethylene−MA exchange, especially meaningful for the mechanistic analysis, was also measured and found to be the fastest of the three exchange processes (Table 3, entry 6, and Figure 6c).

Discussion

The applicability of the Curtin−Hammet treatment for the cyclophane Pd(II) catalyst system given by eq 1 is in question on the basis of the results of rate measurements for ethylene exchange and for the ethylene−MA pair. Ethylene exchange for the cyclophane catalyst is approximately 100 times slower than the acyclic catalyst at 35 °C, but the discrepancy of the rates of exchange with other olefins appears to be even larger. To arrive at more meaningful energetic parameters and to permit the estimation of exchange rates under realistic polymerization conditions, approximate values for the second-order rate constants of exchange processes were calculated. From eqs 2 and 3, both k_2 and k_{-2} can be approximated as eqs 12 and 13. The above-determined values of the equilibrium constant K_{eq}, rewritten in the form of eq 14, and use of the predetermined sum $k_1 + k_{-1}$ as a boundary condition then permit the calculation of k_2 and k_{-2}.

$$k_2 \approx \frac{k_1}{[L_B]} \tag{12}$$

$$k_{-2} \approx \frac{k_{-1}}{[L_A]} \tag{13}$$

$$K_{eq} = \frac{k_2}{k_{-2}} \approx \frac{k_1[L_A]}{k_{-1}[L_B]} \tag{14}$$

Values of the second-order rate constants for the exchange of ethylene−MS, MS−MA, and ethylene−MA pairs are shown in Table 4. At low temperatures, exchange rates are fast enough relative to migratory insertion that they can be measured without complication. Because of the strongly negative entropy of activation of associative ligand exchange, in contrast to insertion, insertion rates likely become faster at polymerization temperature. Assuming an entropy of activation of −30 cal/mol*K based on the results of the ethylene exchange experiments, the free energy barrier of exchange at the polymerization temperature of 35 °C were estimated. From these results, exchange between ethylene and the other olefins appears significantly slower than the exchange of ethylene, even in the favorable reverse direction. For example, values of k_{-2} for ethylene−MS and ethylene−MA, 4.6 s^{-1} M^{-1} and 12 s^{-1} M^{-1}, respectively, are less than the ethylene exchange rate constant of 63 s^{-1} M^{-1}. Steric hindrance as a result of the larger olefins is a likely factor leading to reduced associative ligand exchange. Comparisons between the estimated rate constants of exchange processes and the olefin insertion rate constants previously determined are also tabulated in Table 4. In addition, the actual rates were estimated under typical copolymerization conditions using the given rate expressions. These calculations suggest that the rate of ethylene−MA exchange is of the same order of magnitude as the rates of olefin insertion for the cyclophane system. These rates are calculated under the assumption that the complexes reach equilibrium as measured above. Since there is likely a larger quantity of MA complex due to slow equilibration with the ethylene complex, as elaborated below, the rates of MA insertion with respect to ethylene insertion shown in Table 4 can be taken as a minimum value.

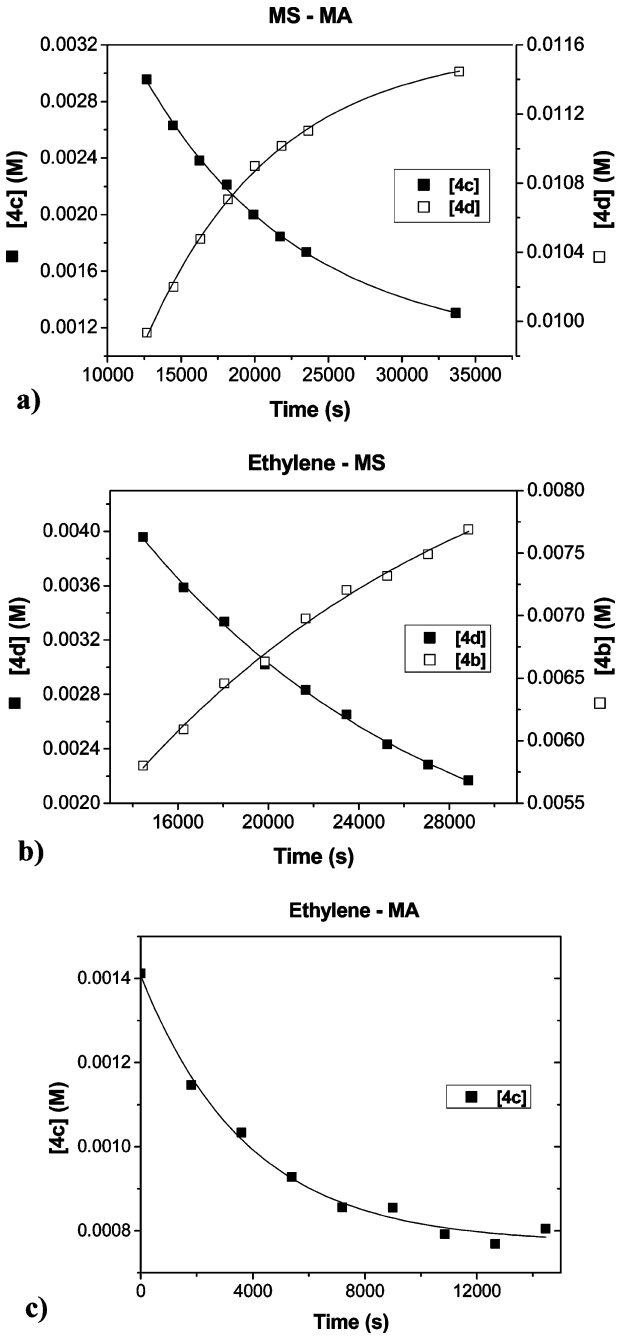

Figure 6. Plots and first-order exponential fits of Pd−olefin adduct concentrations in equilibrium measurements of (a) MA and MS cyclophane adducts **4c** and **4d** at 202 K, (b) ethylene and MS cyclophane adducts **4b** and **4d** at 202 K, and (c) MA adduct **4c** in equilibrium measurements with ethylene at 196 K.

On the basis of the energetic values calculated in Table 4, a free energy diagram of the copolymerization of ethylene and MA is constructed (Figure 7). Whereas the overall energetic landscape of the cyclophane system has some similarity to the acyclic case, the cyclophane system has significantly larger barrier to equilibration of the olefin comonomers. The activation barrier for displacement of ethylene by MA is 20.6 kcal/mol. On the basis of the presumptive 5-coordinate trigonal bipyramidal model of the transition state in associative ligand exchange,[31] the transition state structure **5** is proposed. Due to the steric bulkiness of the cyclophane ligand, formation of the 5-coordinate transition state is very unfavorable, leading to much higher activation energy.

By inspection of Figure 7, it is apparent that the fast-equilibrium prerequisite for the Curtin−Hammett scenario does not exist in the cyclophane system. In fact, our data suggest that the activation energy of equilibration in either direction is larger than both MA and ethylene insertion at polymerization temperature, and that the transition state of ligand exchange is likely the energetic maxima of the system. The barrier for displacement by MA of ethylene adduct **4b** is disfavored by about 2 kcal/mol over ethylene insertion. This means that complex **4b** present will be directed toward insertion versus MA displacement by a factor of $k_E/(k_2[MA]) \approx 7.2$, under the polymerization conditions of Table 1, entry 7. Regarding MA complex **4c**, the barriers to MA insertion and displacement by ethylene are comparable ($k_A/(k_{-2}[C_2H_4]) \approx 1.4$ under the same conditions) meaning at least a substantial amount of **4c** will undergo MA insertion before displacement by ethylene.

The olefin complexes are being continuously created by the complexation of free olefins to the alkyl agostic polymerization intermediate **6** that results after each monomer insertion. As a result, the olefin complexes form in amounts dependent on the rates of ethylene versus MA trapping of the alkyl agostic intermediate **6**. To the best of our knowledge, rate constants for the trapping of MA and ethylene have never been accurately

(31) Shultz, L. H.; Tempel, D. J.; Brookhart, M. *J. Am. Chem. Soc.* **2001**, *123*, 11539–11555.

Table 3. Equilibration of Olefin Complexation in [(N^N)PdMe(L)]SbF_6[a]

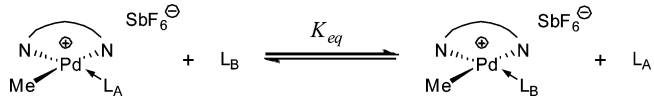

entry	ligand series	L_A-L_B	T (K)	K_{eq}	ΔG (kcal/mol)	k_{ex} (s^{-1})[b,c]
1	**3**	MS−MA	178	$(1.8 \pm 0.4) \times 10^{-4}$[d]	3.1 ± 0.1	fast[e]
2	**3**	C_2H_4−MS	202	$(7.1 \pm 1.4) \times 10^{-3}$	2.0 ± 0.1	fast
3	**3**	C_2H_4 −MA	178	$(1.3 \pm 0.4) \times 10^{-6}$[d]	5.1 ± 0.2	fast
4	**4**	MS−MA	202	$(3.0 \pm 1.1) \times 10^{-3}$[c]	2.3 ± 0.1	$(1.0 \pm 0.1) \times 10^{-4}$
5	**4**	C_2H_4−MS	202	$(9.0 \pm 1.5) \times 10^{-3}$[c]	1.9 ± 0.1	$(6.8 \pm 0.2) \times 10^{-5}$
6	**4**	C_2H_4−MA	196[f]	$(2.7 \pm 1.7) \times 10^{-5}$[g]	4.2 ± 0.2	$(2.6 \pm 2.0) \times 10^{-4}$

[a] Determined by ^{1}H NMR. Solvent = CD_2Cl_2. [b] $k_{ex} = k_1 + k_{-1}$. [c] Determined by first-order exponential fitting of the equilibration plots. [d] From ref 15 for the catalyst bearing ligand ArN=C(H)−C(H)=NAr, Ar = 2,6-*i*-$Pr_2C_6H_3$. [e] Too fast to measure. [f] Temperature at which exchange rate was determined. [g] Calculated from the product of entries 5 and 6.

Table 4. Comparison of the Rates of Insertion and Exchange Processes Related to the Copolymerization of MA and Ethylene by the Cyclophane Catalyst[a]

process	rate constants at 35 °C[b]	$\Delta G^{\ddagger}$ (kcal/mol) at 35 °C[b]	rate law expression	typical rate at polymerization conditions[c]
migratory insertion of ethylene	$k_1 = 0.27\ s^{-1}$[d]	18.9 ± 0.8[d]	$k_E[Pd(C_2H_4)]$	5.4×10^{-5} M/s
migratory insertion of MA	$k_1 = 17\ s^{-1}$[d]	16.3 ± 0.6[d]	$k_A[Pd(MA)]$	8.5×10^{-6} M/s
ethylene exchange	$k_2 = 63\ s^{-1}\ M^{-1}$[e]	15.5 ± 0.4[e]	$2k_2[Pd(C_2H_4)][C_2H_4]$	0.013 M/s
ethylene−MS exchange[f]	$k_2 = 0.21\ s^{-1}\ M^{-1}$[g,h] $k_{-2} = 4.6\ s^{-1}\ M^{-1}$[g,i]	19.0 ± 1.0[j]	$k_2[Pd(C_2H_4)][MS] = k_{-2}[Pd(MS)][C_2H_4]$	N/A
ethylene−MA exchange[f]	$k_2 = 0.015\ s^{-1}\ M^{-1}$[g,h] $k_{-2} = 12\ s^{-1}\ M^{-1}$[g,i]	20.6 ± 1.4[j]	$k_2[Pd(C_2H_4)][MA] = k_{-2}[Pd(MA)][C_2H_4]$	7.0×10^{-6} M/s

[a] Conditions of Table 1, entry 7: [Pd] = 0.20 mM, $[C_2H_4]$ = 1 M at 88 psi (ref 15), [MA] = 2.5 M. [b] Calculated by extrapolation to 35 °C from low temperature ^{1}H NMR experimental measurements. k_1 and k_2 designate rate constants of first- and second-order processes, respectively. [c] Under equilibrium conditions. Rate expressions written for the disappearance of equilibrating Pd complex, e.g. in eq 2, or inserting Pd complex. [d] Extrapolated from activation parameters presented in Table 1 of ref 22. [e] Extrapolated from activation parameters calculated from the results of EXSY NMR experiments. [f] Displacement of ethylene denotes the forward direction. [g] Estimated from equilibrium constants and pseudo-first-order rate constants found in Table 3. [h] Forward rate constant. [i] Reverse rate constant. [j] Barrier in forward direction.

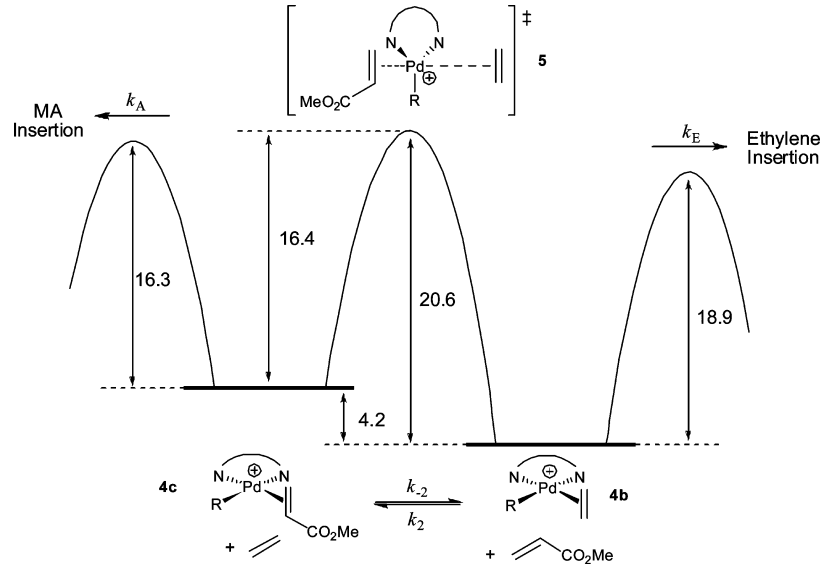

Figure 7. Free energy diagram of ethylene/MA copolymerizations at 35 °C by the cyclophane catalyst. Energetic values are given in kcal/mol.

measured but must be very fast. Spectroscopic studies routinely detect the alkyl olefin complexes such as **4b** and **c**, but the agostic intermediates **6** are never observed in the presence of free olefins. Their energies are normally shown as being far higher than that of the olefin complexes, which are considered to be the polymerization resting states.[15,19,31] In computational studies by Ziegler and co-workers, for example, the complexation of ethylene to the agostic intermediate **6** was calculated to be favored by 16.4 kcal/mol.[16] From Hammond's postulate, the transition states of ethylene and MA olefin trapping will more closely resemble the structure and energy of the common intermediate **6** than the respective olefin complexes; thus, the energy barriers and rate constants to trapping should be approximately the same for both olefins (Figure 8). Because the concentrations of free olefins in solution will affect the trapping rates, comonomer loading will have a large effect on the concentrations of the olefin complexes.

Because of the smaller energy difference in the trapping barriers and the slow exchange of olefins for the cyclophane catalyst, the MA complex will be generated in amounts larger than would be

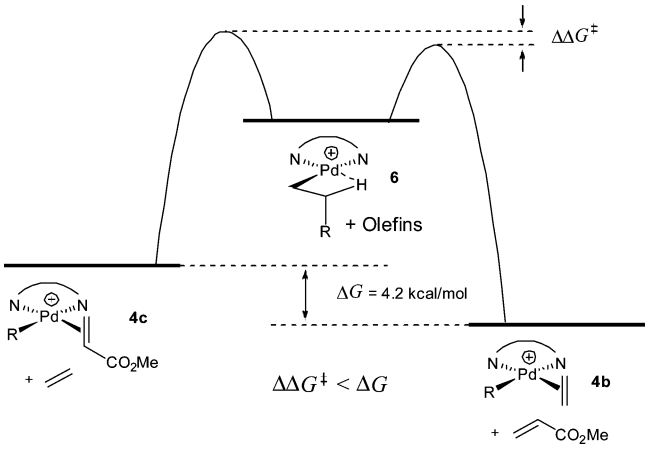

Figure 8. Free energy diagram of the trapping of ethylene and MA by alkyl agostic intermediate **6**.

permitted by olefin equilibrium ($\Delta\Delta G^{\ddagger} < \Delta G$, Figure 8). This situation contrasts dramatically with that of the acyclic catalyst, where the concentrations of the olefin complexes should always exist at their equilibrium levels because of rapid exchange. In the so-called kinetic quenching scenario,[32] the opposite condition from the Curtin−Hammet scenario in which insertion is much faster than exchange, the incorporation of acrylate is dependent solely on the ratio k_A/k_E. In the cyclophane system, however, the exchange rates are likely within an order of magnitude of the insertion rates, constituting an intermediate situation in between the Curtin−Hammett and kinetic quenching scenarios. This intermediate case cannot be treated by a simple analytical solution.

The acyclic catalyst exhibits high selectivity toward ethylene insertion because of the greatly favored complexation of ethylene over acrylate comonomers. In the cyclophane-based catalyst, however, this selectivity is dramatically reduced, allowing for the insertion of monomers that bind weakly to the metal. Because of the small difference in olefin trapping barriers and the large barrier for olefin exchange, enrichment in acrylate complex concentration above what would be permitted by relative olefin binding strengths occurs. Since olefin exchange rates are less than insertion rates, the concentrations of olefin complexes are unable to return to their equilibrium concentrations. Therefore, a disproportionately large amount of acrylate complex undergoes insertion without the establishment of equilibrium. In this manner, the structure of the cyclophane ligand is able to kinetically control comonomer incorporation ratios.

Conclusions

The copolymerization of ethylene with methyl and *tert*-butyl acrylate using the cyclophane-based Pd(II) α-diimine catalyst led to dramatically higher polar monomer incorporation compared to what was observed with the acyclic catalyst. A detailed mechanistic investigation was carried out to determine the cause of this unusual behavior. Efforts were devised to analyze the applicability of the existing Curtin−Hammett fast olefin exchange scenario for acrylate incorporation with the cyclophane catalyst. Key findings from mechanistic studies of the cyclophane-based catalyst are as follows:

(1) In ligand binding studies, a large preference for the complexation of nitriles compared to that of olefins was observed. This effect was attributed to the steric bulk of the cyclophane ligand disrupting the binding orientation of olefins and thus destabilizing η^2-π-type olefin complexes as compared to η^1 σ-donating complexes.

(2) Ethylene exchange, monitored by two-dimensional EXSY NMR methods, was found to proceed over 100 times more slowly than with the acyclic catalyst. From determination of the temperature dependence on ethylene exchange, the entropy of activation was found to be almost the same for the two catalysts. The value of −33 cal/mol*K was consistent with an associative mechanism of olefin exchange. The enthalpy of activation of the cyclophane catalyst, however, was found to be 2.8 kcal/mol higher than the acyclic catalyst. This increase in the barrier height was attributed to the increased steric bulk of the cyclophane ligand, which obstructs access of the incoming ligand to the axial coordination sites on the metal.

(3) Dramatically reduced equilibration rates of cyclophane-bound olefin adducts were observed. The rate constants of exchange of ethylene with other olefins, most importantly MA, were determined by exponential curve fitting to the time-dependence of equilibrating olefin concentrations. The pseudo-first-order rate constants for the displacement of ethylene by MA were calculated to be 0.015 and 12 s^{-1} M^{-1} at 35 °C in the forward and reverse directions, respectively. Rates of ligand exchange are diminished to be on the order of the monomer insertion rates. This observation is also attributed to the steric bulk of the cyclophane ligand blocking the metal axial sites, inhibiting associative ligand substitution.

(4) Equilibrium constants of ethylene and MA complexation were also determined by exponential fitting to the olefin concentration curves. The complexation of MA was favored by 3 to 4 times in the cyclophane catalyst as compared to the acyclic catalyst. Although this would normally be expected to contribute to the relatively high incorporation of MA in the cyclophane catalyst, the slow equilibration rates of the cyclophane catalyst make the Curtin−Hammet scenario inapplicable to this system.

(5) The second-order rate constants and energy barriers for the exchange of ethylene with MA were calculated following the pseudo-first-order approximation. Exchange barrier heights were found to be similar to or to even exceed the insertion barrier heights.

The loss of the prerequisite of fast monomer equilibration relative to monomer insertion thus renders the Curtin−Hammett approximation invalid for the cyclophane system. The net result is significant loss of selectivity of the catalyst for the preferential incorporation of strongly binding olefins. Instead, the relative trapping rates of MA and ethylene to the alkyl agostic polymerization intermediate are believed to factor significantly in the resulting comonomer incorporation ratios. These results have successfully demonstrated the control of the composition of polar olefin copolymers by kinetic regulation of polymerization processes using a ligand with a unique cyclophane structure.

Acknowledgment. We thank the National Science Foundation (Chem-0456719, Chem-0723497, DMR-0703988) for funding. C.P. acknowledges the Allergan Graduate Fellowship, the UCI Department of Chemistry, and Joan Rowland for financial support. We also thank Dr. Phil Dennison for valuable NMR assistance and Prof. Keith Woerpel and Dr. Fiona Lin for helpful discussions.

Supporting Information Available: Details of the synthesis and characterization of complexes, data on EXSY experiments on **4b** at various mixing times, and concentration data for olefin equilibration experiments. This material is available free of charge via the Internet at http://pubs.acs.org.

(32) Seeman, J. I. *Chem. Rev.* **1983**, *83*, 83–134.

JA904471V